

Many-body theory for luminescence spectra in high-density electron-hole systems

T. J. Inagaki* and M. Aihara

Graduate School of Materials Science, Nara Institute of Science and Technology, Ikoma, Nara 630-0101, Japan

(Received 7 August 2001; revised manuscript received 12 November 2001; published 15 May 2002)

We present a unified theory for the luminescence spectra in highly excited semiconductors, which is applicable throughout the whole density regime including the electron-hole ($e-h$) BCS state and the excitonic Bose-Einstein condensate. The calculated spectra clearly show the crossover behavior between the $e-h$ BCS state and the excitonic Bose-Einstein condensate. The analysis is based on the generalized random-phase approximation combined with the Bethe-Salpeter equation. This approach allows us to consider the strong and weak $e-h$ pair correlations on the same basis. In particular, we find that the broad spectral component arising from the carrier recombination in the $e-h$ BCS state splits into the P and P_2 lines with decreasing $e-h$ density. This behavior can be predicted neither by the BCS-like mean-field theory nor by the interacting Boson model. The result agrees with a recent noteworthy experiment for the strongly excited ZnO, where the ultraviolet laser emission was observed at room temperature.

DOI: 10.1103/PhysRevB.65.205204

PACS number(s): 71.35.-y, 78.55.-m, 78.20.-e

I. INTRODUCTION

Many-body effects in photoexcited semiconductors have attracted considerable attention in the last three decades. The system exhibits various states by changing the frequency and intensity of excitation light. The Bose-Einstein condensation (BEC) of excitons is particularly interesting, and has been extensively studied both theoretically and experimentally.¹ However, we still do not have conclusive experiments for direct observation of the excitonic BEC because of the several complicated experimental situations such as phonon effect,² spatial inhomogeneity of exciton density, band anisotropy, finite lifetime of excitons, and so forth. Recent developments in experimental techniques allows us to observe remarkable phenomena suggesting the generation of macroscopic quantum coherence in semiconductors. In particular, the anomalous exciton transport phenomena observed in Cu_2O (Ref. 3) and BiI_3 (Ref. 4) are typical examples of them. These phenomena become more significant with increasing electron-hole $e-h$ density, and this property is in a marked contrast to the simple ballistic exciton propagation or conventional diffusive exciton transport.

When we theoretically analyze many-body effects in high-density $e-h$ systems induced by an intense light, conventional approaches based either on the weak interacting Boson model⁵ or on the BCS-like mean-field theory⁶ are not appropriate. This is because the mean interparticle distance is often of the same order as the radius of a bound $e-h$ pair in practical experimental situations. We have to incorporate the state-filling effect, the band-gap renormalization (BGR) and the quantum fluctuation associated with the center-of-mass motion of $e-h$ pairs on the same footing.

The system exhibits a crossover between the excitonic BEC state in relatively low densities and the $e-h$ BCS state in very high densities.⁷ We should remind that physical properties of these states are qualitatively different from each other. Namely, in the $e-h$ BCS state, the relative motion of $e-h$ pairs is relevant and the order parameter is the BCS-like gap at the quasi-Fermi level. In the excitonic BEC state, on the other hand, the center-of-mass motion of $e-h$ pairs deter-

mines the macroscopic quantum coherence and the order parameter is the density of condensed excitons.

Apart from the photoexcited semiconductors, the BCS-BEC crossover has long been discussed in a variety of physical contexts including superconductivity,⁸ nuclear matter,⁹ and superfluid ^3He (Ref. 10). In particular, much attention has been focused on the BCS-BEC crossover in connection with high- T_c cuprate superconductivity,^{11,12} where a pseudogap structure is observed in the normal-state density-of-states for underdoped cuprates almost up to room temperature. It is known that the coherence length of high- T_c superconductor is the same order as the mean interparticle distance.¹³ This fact is in contrast with the conventional superconductors where the Cooper pairs are strongly overlapping in real space. The optically excited $e-h$ system has a marked advantage to investigate the BCS-BEC crossover because the macroscopic quantum state can easily be controlled without changing the composition of materials.

Recently, a microscopic theory for time-resolved luminescence spectra has been proposed to study the buildup of the exciton luminescence during the plasma cooling processes.¹⁴ The theory is further elaborated to study the secondary emission, the hot luminescence, and the exciton formation under the photonic environments.¹⁵ This attempt is particularly interesting because the spontaneous generation of the macroscopic coherence in photoexcited semiconductors is one of the fundamental interests as in the case of the BEC in cold atomic vapors.¹⁶

In this paper, we study the luminescence spectra from the macroscopic quantum state in highly excited semiconductors; the theory is applicable throughout the whole densities including the $e-h$ BCS state in very high densities and the excitonic BEC in relatively low densities. The analysis is based on the BCS-like pairing theory combined with the Bethe-Salpeter equation¹⁷ for the $e-h$ pair correlation function. This formulation allows us to incorporate the state-filling effect, the band-gap renormalization, and the weak ($e-h$ Cooper pair formation) and strong (exciton formation) pair correlations on the same basis. This analysis is closely related to those in Refs. 18 and 19, where the absorption

spectra for condensed exciton system is analyzed by numerically solving the ladder BS equation. In the present theory, we incorporate the collective phase fluctuation associated with the center-of-mass motion of e - h pairs by the generalized random-phase approximation (GRPA).²⁰ In addition, the present theory considers the many-exciton correlations such as the inelastic exciton-exciton interaction; the many-exciton correlation is one of the main interests in the present semiconductor spectroscopy, and this effect can be discussed neither with the semiconductor Bloch equation²¹ nor on the semiconductor luminescence equation proposed by Kira *et al.*¹⁴

The calculated spectra exhibit the BCS-BEC crossover that can be analyzed neither by the BCS-like mean-field theory nor by the interacting Boson model. In particular, the present theory clearly shows that the broad emission band, arising from the pair recombination in the e - h BCS state, splits into the P and P_2 lines with decreasing carrier density. Here the P (P_2) line arises from the radiative recombination of an exciton assisted by the excitation of another exciton from the $1S$ to ionization-continuum ($2S$) state. In addition, we find in the calculated spectra the weak emission line above the quasichemical potential of e - h pairs originating from the recombination of Bogoliubov quasiparticle pairs generated by the collective phase fluctuation.

We analyze the density dependence of the band-gap shift due to the band-gap renormalization, and find that the present theory agrees very well with experiments for ZnO and CuCl. Furthermore, we discuss the density dependences of each spectral component on e - h density. The present theory shows that the linear (quadratic) density dependence of the peak intensity of exciton (P_2) line saturates with increasing e - h density. It should be stressed that, in low densities, the present theory enables us to calculate the coherent exciton emission, P and P_2 lines with the same basic equation.

From the point of view of the BCS-BEC crossover, the present work is regarded as an important attempt to clarify the phenomenon by using response functions. It should be remarked that only the thermodynamic properties have been studied in the previous works on this subject.

The present theory is also important from application point of view. The optical properties of wide band-gap II-VI semiconductors have attracted much attention following the development of the short-wavelength semiconductor laser diodes. In particular, the room-temperature ultraviolet laser emission from the self-assembled ZnO microcrystallite thin film²² is interesting, because other wide band-gap materials, such as ZnSe, exhibit the ultraviolet laser emission only when the system is at sufficiently low temperatures (below 100 K). This laser emission arises from the P -line, and the many-body effects play an essential role in the lasing mechanism. Therefore, elaborating the quantitative theory for high-density e - h system is particularly important to design novel optical devices based on the wide band-gap materials. The present theory is a quantitative theory for luminescence spectra of highly excited semiconductors, which provides us with a theoretical basis to design novel short-wavelength optical devices using wide band-gap materials.

The paper is organized as follows. In Sec. II, we derive the BS equation for the e - h pair correlation function within the quasistatically screened ladder approximation. We introduce the Bogoliubov quasiparticle operators to take into account the e - h pair correlation. The numerical analysis and comparison with experiments are given in Sec. III. We discuss in Sec. III A the dependence of the renormalized band-gap on the e - h density, and compare the corresponding experiments for ZnO (Refs. 23,24) and CuCl.²⁵ In Sec. III B, the e - h pair correlation and the BCS-like gap formation are discussed by analyzing the density dependences of the e - h pair excitation energy and the e - h pair wave function with zero center-of-mass momentum. We show in Sec. III C the calculated luminescence spectra and compare them with those given by the BCS-like mean-field theory, the GRPA analysis, and the corresponding experiment for ZnO.²⁶ We analyze in Sec. III D the density dependences of the luminescence intensity and the spectral position for each spectral component. Conclusions are given in Sec. IV. Finally, we show in the three appendixes the derivation of the several formulas that are used to evaluate the ladder BS equation.

II. FORMULATION

A. Model Hamiltonian

We consider a three-dimensional e - h system in a direct-gap semiconductor at $T=0$, which consists of an isotropic, nondegenerate parabolic conduction and valence bands with identical electron and hole effective masses; the analysis for different effective masses will be given in a forthcoming paper.²⁷ The repulsive interactions between electrons and between holes as well as the e - h attractive interaction are taken into account. The spin degrees of freedom are neglected to focus our attention on the essential point of the BCS-BEC crossover. We consider that the system is in a quasistationary state given by the quasichemical potential μ of the e - h pairs. The Hamiltonian is expressed in terms of annihilation operators of electrons (c_p) and holes (d_p) as follows:

$$H_{\text{mat}} = \sum_{\mathbf{k}} \{ \varepsilon_{\mathbf{k}}^e c_{\mathbf{k}}^\dagger c_{\mathbf{k}} + \varepsilon_{\mathbf{k}}^h d_{-\mathbf{k}}^\dagger d_{-\mathbf{k}} \} + \frac{1}{2} \sum_{k,p,q} V_q \{ c_{k+q}^\dagger c_{p-q}^\dagger c_p c_k + d_{k+q}^\dagger d_{p-q}^\dagger d_p d_k - 2c_{k+q}^\dagger c_k d_{p-q}^\dagger d_p \}. \quad (1)$$

The single-particle energies of electrons and holes are expressed in terms of their effective mass m as $\varepsilon_{\mathbf{k}}^e = k^2/(2m) + E_g - \mu/2$ and $\varepsilon_{\mathbf{k}}^h = k^2/(2m) - \mu/2$, respectively, where E_g is the band-gap energy. The Coulomb interaction is written as $V_q = 4\pi e^2/(\epsilon_0 q^2)$, where ϵ_0 is the background dielectric constant of the unexcited crystal.

B. BCS-like gap equation for e - h systems

We rewrite Eq. (1) with respect to Bogoliubov quasiparticle operators $\alpha_{\mathbf{k}}$ and $\beta_{\mathbf{k}}$ to consider the e - h pair correlation. The annihilation operators for Bogoliubov quasiparticles are defined by the Bogoliubov transformation,

$$\begin{aligned} c_k &= u_k \alpha_k + v_k \beta_{-k}^\dagger, \\ d_{-k} &= u_k \beta_{-k} - v_k \alpha_k^\dagger, \end{aligned} \quad (2)$$

where the Bogoliubov parameters u_k and v_k are subject to the unitarity condition, $u_k^2 + v_k^2 = 1$. For later convenience, we introduce the coherence factors by

$$\begin{aligned} C_{k,p}^{(0)} &= u_k u_p + v_k v_p, \\ C_{k,p}^{(1)} &= u_k v_p + v_k u_p, \\ C_{k,p}^{(2)} &= u_k u_p - v_k v_p, \\ C_{k,p}^{(3)} &= u_k v_p - v_k u_p, \end{aligned} \quad (3)$$

and the two-component operator in Nambu representation by

$$\phi_k = \begin{pmatrix} \alpha_k^\dagger \\ \beta_{-k} \end{pmatrix}, \quad \phi_k^\dagger = (\alpha_k, \beta_{-k}^\dagger). \quad (4)$$

The e - h Hamiltonian H_{mat} is then expressed as follows:

$$\begin{aligned} H_{\text{mat}} &= \sum_k \mathcal{E}_k^\mu (\phi_k^\dagger \boldsymbol{\tau}_\mu \phi_k) + \frac{1}{2} \sum_{k,p,q} W_{k,p}^{\mu,\nu}(\mathbf{q}) (\phi_{k+q}^\dagger \boldsymbol{\tau}_\mu \phi_k) \\ &\quad \times (\phi_{p-q}^\dagger \boldsymbol{\tau}_\nu \phi_p), \end{aligned} \quad (5)$$

where $\boldsymbol{\tau}_0$ and $\boldsymbol{\tau}_j$ ($j=1,2,3$) are the 2×2 unit matrix and Pauli matrix, respectively. In the following analysis, we use the summation convention with respect to indices μ and ν ($\mu, \nu = 0, 1, \dots, 3$), unless otherwise stated. In Eq. (5), \mathcal{E}_k^μ is written as follows:

$$\begin{aligned} \mathcal{E}_k^0 &= \frac{1}{2} (\varepsilon_k^e - \varepsilon_k^h) = 0, \\ \mathcal{E}_k^1 &= \frac{1}{2} \left(\varepsilon_k^e + \varepsilon_k^h - \sum_q V_q \right) C_{k,k}^{(1)}, \\ \mathcal{E}_k^2 &= 0, \\ \mathcal{E}_k^3 &= \frac{1}{2} \left(\varepsilon_k^e + \varepsilon_k^h - \sum_q V_q \right) C_{k,k}^{(2)}. \end{aligned} \quad (6)$$

Furthermore, the quantity $W_{k,p}^{\mu,\nu}(\mathbf{q})$ is written as follows:

$$\begin{aligned} &W_{k,p}^{\mu,\nu}(\mathbf{q}) \\ &= V_q \begin{pmatrix} C_{k+q,k}^{(0)} C_{p-q,p}^{(0)} & 0 & i C_{k+q,k}^{(0)} C_{p-q,p}^{(3)} & 0 \\ 0 & 0 & 0 & 0 \\ i C_{k+q,k}^{(3)} C_{p-q,p}^{(0)} & 0 & -C_{k+q,k}^{(3)} C_{p-q,p}^{(3)} & 0 \\ 0 & 0 & 0 & 0 \end{pmatrix}_{\mu,\nu}. \end{aligned} \quad (7)$$

The Bogoliubov parameters are determined by the variational method; we minimize the expectation value of the Hamiltonian, $\langle H_{\text{mat}} \rangle_0$, under the charge neutrality condition, $\sum_k \{ \langle c_k^\dagger c_k \rangle_0 + \langle d_{-k}^\dagger d_{-k} \rangle_0 \} = 0$, where $\langle \dots \rangle_0$ stands for the

expectation value with respect to the Bogoliubov quasiparticle vacuum. A straightforward calculation gives

$$u_k^2 = \frac{1}{2} \left(1 + \frac{\zeta_k}{E_k} \right), \quad v_k^2 = \frac{1}{2} \left(1 - \frac{\zeta_k}{E_k} \right), \quad (8)$$

where ζ_k , Δ_k , and $E_k \equiv \sqrt{\zeta_k^2 + \Delta_k^2}$ are the renormalized energy of e - h pairs, the BCS-like energy gap, and the excitation energy of a pair of Bogoliubov quasiparticles, respectively. The quantities ζ_k and Δ_k are determined by solving the following self-consistent equations:

$$\begin{aligned} \zeta_k &= \left(\frac{k^2}{2m^*} + E_g - \mu \right) - 2 \sum_p V_{k-p} v_p^2 \\ &= \left(\frac{k^2}{2m^*} + E_g - \mu \right) - \sum_p V_{k-p} \left(1 - \frac{\zeta_p}{E_p} \right), \end{aligned} \quad (9a)$$

$$\Delta_k = -4 \sum_p V_{k-p} u_p v_p = -2 \sum_p V_{k-p} \frac{\Delta_p}{E_p}, \quad (9b)$$

where $m^* \equiv m/2$ is the reduced mass of e - h pairs. The second term on the right-hand side of Eq. (9a) expresses the band renormalization effect arising from the electron (hole) exchange interaction, and Eq. (9b) is the BCS-like gap equation that describes the spontaneous generation of the BCS-like energy gap.

In order to obtain physical insight into the BCS-like gap equation, we express Eq. (9) in terms of the e - h pair wave function with zero center-of-mass momentum, $\psi_k = \langle c_k d_{-k} \rangle = \Delta_k / (2E_k)$. Making use of Eq. (8), the BCS-like gap equation can be rewritten as

$$\begin{aligned} &\left\{ \frac{k^2}{2m^*} + E_g - \mu - 2 \sum_p V_{k-p} v_p^2 \right\} \psi_k - (1 - 2v_k^2) \\ &\quad \times \sum_p V_{k-p} \psi_p = 0. \end{aligned} \quad (10)$$

Equation (10) is reduced to the Wannier equation in the limit of low e - h density, because $v_k^2 = \langle c_k^\dagger c_k \rangle_0 = \langle d_{-k}^\dagger d_{-k} \rangle_0$ is the distribution function for electrons and holes. Therefore the BCS-like pair theory is able to properly describe the relative wave function of excitons in the low-density case as well as the BCS-like pair states in the high-density case as discussed in Refs. 6,8,28,29,31.

C. Linear optical response

In order to calculate the luminescence spectra, we consider the radiation-matter coupled system described by the following Hamiltonian:

$$H_{\text{tot}} = H_{\text{rad}} + H_{\text{mat}} + H_{\text{int}}, \quad (11)$$

where H_{rad} and H_{int} are the Hamiltonians for radiation field and for the interaction between radiation and carriers, respectively; H_{mat} is the e - h Hamiltonian given by Eq. (1). H_{rad} and H_{int} are written in terms of annihilation operator for photons b as follows:

$$H_{\text{rad}} = \omega b^\dagger b, \quad (12a)$$

$$H_{\text{int}} = \sum_{\mathbf{k}} \{g_{\mathbf{k}} b^\dagger c_{\mathbf{k}} d_{-\mathbf{k}} + g_{\mathbf{k}}^* d_{-\mathbf{k}}^\dagger c_{\mathbf{k}}^\dagger b\}, \quad (12b)$$

where ω and $g_{\mathbf{k}}$ are the frequency of the light and radiation-matter coupling constant, respectively.

We then consider the equation of motion for the expectation value of the photon number operator, $N(t) = b^\dagger(t)b(t)$. A perturbative calculation with respect to H_{int} gives

$$\frac{d}{dt} \langle N(t) \rangle = \Pi^<(\omega) \langle N(t) + 1 \rangle - \Pi^>(\omega) \langle N(t) \rangle, \quad (13)$$

where $\langle \dots \rangle$ indicates the expectation value with respect to the ground state of H_{tot} . The quantities $\Pi^<(\omega)$ and $\Pi^>(\omega)$ are the emission and the absorption rate of photons, respectively, and they are expressed in terms of electron and hole operators as follows:

$$\begin{aligned} \Pi^>(\omega) &= \sum_{\mathbf{k}, \mathbf{p}} g_{\mathbf{k}}^* g_{\mathbf{p}} \int_0^\infty dt \langle d_{-\mathbf{p}}(t) c_{\mathbf{p}}(t) c_{\mathbf{k}}^\dagger(0) d_{-\mathbf{k}}^\dagger(0) \rangle_0 e^{i\omega t} + \text{c.c.} \\ &= -2 \text{Im} G^>(\omega - \mu + i\gamma), \end{aligned}$$

$$\begin{aligned} \Pi^<(\omega) &= \sum_{\mathbf{k}, \mathbf{p}} g_{\mathbf{k}}^* g_{\mathbf{p}} \int_0^\infty dt \langle c_{\mathbf{k}}^\dagger(0) d_{-\mathbf{k}}^\dagger(0) d_{-\mathbf{p}}(t) c_{\mathbf{p}}(t) \rangle_0 e^{i\omega t} + \text{c.c.} \\ &= -2 \text{Im} G^<(\omega - \mu + i\gamma), \end{aligned} \quad (14)$$

where γ is the exciton decay constant and $\langle \dots \rangle_0$ stands for the expectation value with respect to the ground state of H_{mat} . The quantities $G^>(\omega)$ and $G^<(\omega)$ are the Fourier transform of the correlation functions defined by

$$iG^>(t) = \Theta(t) \sum_{\mathbf{k}, \mathbf{p}} g_{\mathbf{k}}^* g_{\mathbf{p}} \langle d_{-\mathbf{p}}(t) c_{\mathbf{p}}(t) c_{\mathbf{k}}^\dagger(0) d_{-\mathbf{k}}^\dagger(0) \rangle_0, \quad (15a)$$

$$iG^<(t) = \Theta(t) \sum_{\mathbf{k}, \mathbf{p}} g_{\mathbf{k}}^* g_{\mathbf{p}} \langle c_{\mathbf{k}}^\dagger(0) d_{-\mathbf{k}}^\dagger(0) d_{-\mathbf{p}}(t) c_{\mathbf{p}}(t) \rangle_0. \quad (15b)$$

The luminescence spectrum $I(\omega)$ is given by the spontaneous emission rate, $\Pi^<(\omega)$,

$$I(\omega) = -2 \text{Im} G^<(\omega - \mu + i\gamma). \quad (16)$$

We rewrite Eq. (15b) with respect to the two-component operator Eq. (4) to incorporate the e - h pair correlation. Substituting Eq. (4) into Eq. (15b), we obtain the following formula:

$$\begin{aligned} iG^<(t) &= \frac{1}{4} \Theta(t) \\ &\times \sum_{j,m=1}^3 \sum_{\mathbf{k}, \mathbf{p}} g_{\mathbf{k}}^* g_{\mathbf{p}} \mathbf{K}_{\mathbf{k},j}^\dagger \langle \Phi_j^{0\dagger}(\mathbf{k}, 0) \Phi_m^0(\mathbf{p}, t) \rangle_0 \mathbf{K}_{\mathbf{p},m}, \end{aligned} \quad (17)$$

where $\mathbf{K}_{\mathbf{p},j} = (C_{\mathbf{p},\mathbf{p}}^{(2)}, -i, C_{\mathbf{p},\mathbf{p}}^{(1)})_j$ and

$$\Phi_j^{q\dagger}(\mathbf{p}, t) = \phi_{q+\mathbf{p}}^\dagger(t) \boldsymbol{\tau}_j \phi_{\mathbf{p}}(t). \quad (18)$$

As shown in Appendix A, the operator $\Phi_3^0(\mathbf{p})$ is the constant of motion; therefore the Fourier transform of Eq. (17) is expressed as follows:

$$\begin{aligned} G^<(\omega) &= \frac{I_{\text{coh}}}{4(\omega + i\gamma)} \\ &+ \frac{1}{4} \sum_{j,m=1}^2 \sum_{\mathbf{k}, \mathbf{p}} g_{\mathbf{k}}^* g_{\mathbf{p}} \mathbf{K}_{\mathbf{k},j}^\dagger [\mathcal{G}_{\mathbf{k},\mathbf{p}}(\omega)]_{j,m} \mathbf{K}_{\mathbf{p},m}, \end{aligned} \quad (19a)$$

where $\mathcal{G}_{\mathbf{k},\mathbf{p}}(\omega)$ is the Fourier transform of the following 2×2 matrix correlation function:

$$[\mathcal{G}_{\mathbf{k},\mathbf{p}}(t)]_{j,m} = -i \Theta(t) \langle \Phi_j^{0\dagger}(\mathbf{k}, 0) \Phi_m^0(\mathbf{p}, t) \rangle_0, \quad (19b)$$

and

$$\begin{aligned} I_{\text{coh}} &= \sum_{\mathbf{k}, \mathbf{p}} g_{\mathbf{k}}^* g_{\mathbf{p}} \mathbf{K}_{\mathbf{k},3}^\dagger \langle \Phi_3^{0\dagger}(\mathbf{k}) \Phi_3^0(\mathbf{p}) \rangle_0 \mathbf{K}_{\mathbf{p},3} \\ &+ \sum_{j=1}^2 \sum_{\mathbf{k}, \mathbf{p}} g_{\mathbf{k}}^* g_{\mathbf{p}} \{ \mathbf{K}_{\mathbf{k},j}^\dagger \langle \Phi_j^{0\dagger}(\mathbf{k}) \Phi_3^0(\mathbf{p}) \rangle_0 \mathbf{K}_{\mathbf{p},3} + \text{c.c.} \}. \end{aligned} \quad (19c)$$

In deriving Eq. (19), we should note that the expectation value $\langle \dots \rangle_0$ is evaluated in terms of the quasistationary state. The first term on the right-hand side of Eq. (19a) gives the sharp spectrum at the quasichemical potential of the e - h pairs; this spectral component arises from the coherent spontaneous emission from the macroscopic quantum state. In the coherent emission process, the e - h recombination does not generate Bogoliubov quasiparticles so that the spectral linewidth is merely determined by the lifetime of the e - h pairs. On the other hand, the second term on the right-hand side of Eq. (19a) expresses the incoherent spontaneous emission accompanied by the creation of Bogoliubov quasiparticles; this spectral component reflects the various interesting features arising from the many-body interaction in high-density e - h systems.

As shown in Appendix B, I_{coh} is written as follows:

$$I_{\text{coh}} = \frac{1}{8} \sum_{j=1,2} \sum_{\mathbf{k}, \mathbf{p}} g_{\mathbf{k}}^* g_{\mathbf{p}} C_{\mathbf{k},\mathbf{k}}^{(1)} \langle \Phi_j^{p-k\dagger}(\mathbf{k}) \Phi_j^{p-k}(\mathbf{k}) \rangle_0 C_{\mathbf{p},\mathbf{p}}^{(1)}. \quad (20)$$

We evaluate $\langle \Phi^{p-k\dagger}(\mathbf{k}) \tau_0 \Phi^{p-k}(\mathbf{k}) \rangle_0$ by the GRPA; we show the details of calculation in Appendix C. Substituting Eq. (C9a) into the second term on the right-hand side of Eq. (20), we obtain

$$I_{\text{coh}} = \frac{1}{4} \left| \sum_{\mathbf{k}} g_{\mathbf{k}}^* C_{\mathbf{k},\mathbf{k}}^{(1)} \right|^2 - \sum_{\mathbf{k},\mathbf{p}} g_{\mathbf{k}}^* g_{\mathbf{p}} V_{\mathbf{k}-\mathbf{p}} C_{\mathbf{k},\mathbf{k}}^{(1)} C_{\mathbf{p},\mathbf{p}}^{(1)} C_{\mathbf{k},\mathbf{p}}^{(3)2} \left[\frac{\partial \chi_{\mathbf{k}-\mathbf{p}}(\omega)}{\partial \omega} \right]_{\omega = -E_{\mathbf{k}} - E_{\mathbf{p}}}, \quad (21)$$

where $\chi_q(\omega)$ is the partial screening function defined by Eq. (C10). The first term on the right-hand side of Eq. (21) represents the intensity of the coherent emission evaluated by the BCS-like mean-field theory. On the other hand, the second term on the right-hand side of Eq. (21) reflects the collective phase fluctuation effect associated with the center-of-mass motion of e - h pairs.

D. The Bethe-Salpeter equation for e - h pair-correlation function

Next, let us consider the 2×2 matrix correlation function $\mathcal{G}_{\mathbf{k},\mathbf{p}}(t)$ defined by Eq. (19b). The Fourier transform of $\mathcal{G}_{\mathbf{k},\mathbf{p}}(t)$ satisfies the following BS equation:

$$\left[\mathcal{G}_{\mathbf{p},\mathbf{k}}(\omega) (\omega \tau_0 + 2E_{\mathbf{k}} \tau_3) - \sum_{\mathbf{k}'} V_{\mathbf{k}-\mathbf{k}'} \mathcal{G}_{\mathbf{p},\mathbf{k}'}(\omega) \times (C_{\mathbf{k},\mathbf{k},\mathbf{k}'}^{(0)2} \tau_2 + i C_{\mathbf{k},\mathbf{k},\mathbf{k}'}^{(3)2} \tau_1) \right]_{j,m} = \langle \Phi_j^{0\dagger}(\mathbf{p}) \Phi_m^0(\mathbf{k}) \rangle_0, \quad (22)$$

where $j, m = 1, 2$. This BS equation is obtained by linearizing the equation of motion for $\mathcal{G}_{\mathbf{k},\mathbf{p}}(t)$. The second term on the left-hand side of Eq. (22) expresses the strong e - h pair correlation, where the vertex part proportional to $C_{\mathbf{k},\mathbf{p}}^{(0)2}$ reflects the state-filling effect and the part proportional to $C_{\mathbf{k},\mathbf{p}}^{(3)2}$ arises from the e - h pair correlation. The strong e - h pair correlation gives a significant contribution to the e - h pair recombination with nonzero center-of-mass momentum, and it give rise to the sharp excitonic structures in the luminescence spectrum, which are not obtained with the BCS-like mean-field theory.

As shown in Appendix C, the expectation value on the right-hand side of Eq. (22) can be evaluated by the GRPA. Substituting Eq. (B1) into the expectation value on the right-hand side of Eq. (22), we obtain

$$\langle \Phi_j^{0\dagger}(\mathbf{p}) \Phi_m^0(\mathbf{k}) \rangle_0 = \delta_{\mathbf{p},\mathbf{k}} (\tau_0 + \tau_2)_{j,m} - \frac{1}{2} (\tau_3)_{j,m} \langle \Phi^{p-k\dagger}(\mathbf{k}) \tau_3 \Phi^{p-k}(\mathbf{k}) \rangle_0. \quad (23)$$

Here we used the identity $\text{tr}\{\tau_1 \mathbf{G}^q(\mathbf{k}, \mathbf{k}, \omega)\} = \langle \Phi^{p-k\dagger}(\mathbf{k}) \tau_1 \Phi^{p-k}(\mathbf{k}) \rangle_0 = 0$, where $\mathbf{G}^q(\mathbf{k}, \mathbf{k}, \omega)$ is defined by Eq. (C1). The second term on the right-hand side of Eq.

(23) reflects the collective phase fluctuation from e - h BCS state similar to the Anderson mode in superconductivity. From Eq. (C9b), we find that Eq. (23) turn out to be written as follows:

$$\langle \Phi_j^{0\dagger}(\mathbf{p}) \Phi_m^0(\mathbf{k}) \rangle_0 = \delta_{\mathbf{p},\mathbf{k}} (\tau_0 + \tau_2)_{j,m} - \frac{C_{\mathbf{k},\mathbf{p}}^{(3)2} V_{\mathbf{k}-\mathbf{p}}^s}{E_{\mathbf{k}} + E_{\mathbf{p}}} (\tau_3)_{j,m}. \quad (24)$$

Here we introduced the quasistatically screened Coulomb potential defined by

$$V_{\mathbf{k}-\mathbf{p}}^s = V_{\mathbf{k}-\mathbf{p}} \{1 + 2\chi_{\mathbf{k}-\mathbf{p}}(-E_{\mathbf{k}} - E_{\mathbf{p}})\}, \quad (25)$$

where $\chi_q(\omega)$ is the partial screening function³⁰ defined by Eq. (C10).

E. Screening effect

In the present analysis, we incorporate the screening effect by the quasistatic RPA.²⁸ The BCS-like gap equation Eq. (9) is written as

$$\zeta_{\mathbf{k}} = \left(\frac{k^2}{2m^*} + E_g - \mu \right) - 2 \sum_{\mathbf{p}} V_{\mathbf{k}-\mathbf{p}}^s v_{\mathbf{p}}^2 + \sum_{\mathbf{q}} \{V_{\mathbf{q}}^s - V_{\mathbf{q}}\}, \quad (26a)$$

$$\Delta_{\mathbf{k}} = -4 \sum_{\mathbf{p}} V_{\mathbf{k}-\mathbf{p}}^s \mu_{\mathbf{p}} v_{\mathbf{p}}. \quad (26b)$$

Here, the second term on the right-hand side of Eq. (26a) represents the screened exchange effect, the third term being the Coulomb-hole effect. On the other hand, the BS equation (22) is written as

$$\mathcal{G}_{\mathbf{p},\mathbf{k}}(\omega) (\omega \tau_0 + 2E_{\mathbf{k}} \tau_3) - \sum_{\mathbf{k}'} V_{\mathbf{k}-\mathbf{k}'} \mathcal{G}_{\mathbf{p},\mathbf{k}'}(\omega) (C_{\mathbf{k},\mathbf{k},\mathbf{k}'}^{(0)2} \tau_2 + i C_{\mathbf{k},\mathbf{k},\mathbf{k}'}^{(3)2} \tau_1) = \delta_{\mathbf{p},\mathbf{k}} (\tau_0 + \tau_2) - \tau_3 \frac{C_{\mathbf{k},\mathbf{p}}^{(3)2} V_{\mathbf{k}-\mathbf{p}}^s}{E_{\mathbf{k}} + E_{\mathbf{p}}}. \quad (27)$$

In the present analysis, we employ the tractable expression for the dielectric function given by the single-plasmon-pole approximation,³⁰ which is known to produce relatively good self-energy corrections.^{31,32} In the single-plasmon-pole approximation, the dielectric function is given by

$$\epsilon_{\mathbf{k}}^{-1}(z) = \epsilon_0^{-1} \left(1 + \frac{\omega_{\text{pl}}^2}{z^2 - \omega_{\mathbf{k}}^2} \right), \quad (28)$$

where $\omega_{\text{pl}} = [4\pi n e^2 / (\epsilon_0 m^*)]^{1/2}$ is the plasma frequency, and n is the e - h pair density. The dispersion of the effective plasmon mode is chosen as,³⁰

$$\omega_{\mathbf{k}}^2 = \omega_{\text{pl}}^2 \left(1 + \frac{k^2}{k_{\text{TF}}^2} \right) + G_{\text{eff}}^2, \quad (29)$$

where $k_{\text{TF}} = \{16m^* e^2 / (\pi \epsilon_0)\}^{1/2} (6\pi^2 n)^{1/6}$ is the Thomas-Fermi wave number, and the effective gap

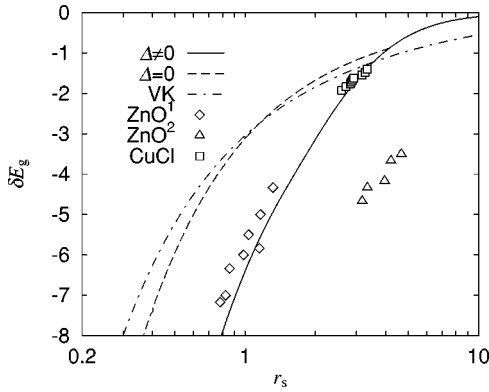


FIG. 1. The BGR as a function of r_s . The present theory gives the solid line and the theory of Vashishta *et al.*³⁴ gives the dashed-dotted line. The dashed line shows the result given by solving Eq. (26) with $\Delta_k=0$. The open diamonds, triangles, and squares represent the experimental results for 233 nm ZnO thin film,²⁴ 55 nm ZnO thin film,²³ and bulk CuCl,²⁵ respectively.

$$G_{\text{eff}} = 2 \min_k E_k \quad (30)$$

is set to the minimum excitation energy of a pair of the Bogoliubov quasiparticles. The partial screening function and its derivative take the following simple forms:

$$\chi_k(\omega) = \frac{\omega_{\text{pl}}^2}{2\omega_k} \left(\frac{1}{\omega - \omega_k} \right), \quad (31)$$

$$\frac{\partial \chi_k(\omega)}{\partial \omega} = - \frac{\omega_{\text{pl}}^2}{2\omega_k} \left(\frac{1}{\omega - \omega_k} \right)^2.$$

III. NUMERICAL ANALYSIS

In the following analysis, we use the units where the exciton binding energy (E_{ex}) and the exciton Bohr radius (a_B) equal unity. As a measure of the e - h density, we employ the dimensionless mean interparticle distance $r_s = \langle r \rangle / a_B = [3/(4\pi n)]^{1/3}$, where n is the e - h density.

A. The band-gap renormalization

Before going into details of the numerical results for the luminescence spectra, we first discuss the band-gap renormalization (self-energy correction) arising from the electron (hole) exchange interaction. This effect plays an important role in several optical phenomena in high-density e - h systems, such as the laser oscillation and the mirrorless optical bistability^{31,33} in semiconductors. In the present analysis, we iteratively solve the BCS-like gap equation (26) for a fixed value of quasichemical potential μ . The band-gap reduction is then evaluated by $\delta E_g = \zeta_{k=0} - E_g + \mu$. In each step of iteration, we need to calculate the e - h density and the effective gap G_{eff} to evaluate the quasistatically screened Coulomb interaction defined by Eq. (25).

Figure 1 shows the calculated δE_g as a function of r_s ; as a reference, we also show the results obtained by solving Eq. (26) with $\Delta_k=0$ and by the phenomenological Vashishta-

Kalia formula.³⁴ Much attention should be paid to the drastic difference between the present theory and other results especially in high e - h densities (small r_s). This large band-gap reduction arises from the BCS-like gap formation; as discussed in Ref. 35, the result obtained by solving Eq. (26) with $\Delta_k=0$ shows almost the same behavior as that of Ref. 34.

We also show in Fig. 1 the experimental results for bulk CuCl (Ref. 25) and ZnO thin film.^{23,24} In Ref. 25, the data for δE_g are obtained by analyzing the threshold pump-light intensity of the plasma emission for various pump-light frequencies. In Refs. 23 and 24, the data for δE_g are obtained by analyzing the low-energy tail of the luminescence and absorption spectra for various pump-light intensities; the sample thickness is 55 nm in Ref. 23 and that in Ref. 24 is 233 nm. In Fig. 1, material parameters are used to evaluate the binding energy and the Bohr radius of a $1S$ exciton; those values for CuCl are $E_{\text{ex}}=213$ meV (Ref. 36) and $a_B=0.7$ nm (Ref. 37), and those for ZnO are $E_{\text{ex}}=59$ meV (Ref. 38) and $a_B=1.8$ nm (Ref. 39).

We find an excellent agreement between the present theory and the experimental data for bulk CuCl and ZnO satisfying the weak confinement condition. We should note that no adjustable parameters are introduced in the theory, and that the universal behavior is found except for strong confinement samples, i.e., the data for different materials fits the same theoretical line. This excellent agreement in Fig. 1 indicates that the BCS-like energy gap is formed in these experiments and plays an important role in the high-density e - h systems.

The importance of the macroscopic coherence generated by the Coulomb interaction was also pointed out in the semiconductor Bloch equation,²¹ which is very useful to analyze various ultrafast optical phenomena including the optical Stark effect.⁴⁰ The results obtained by the present theory are consistent with these studies where the BCS-like mean-field theory is employed. On the other hand, the BGR has extensively been discussed by using GW approximation⁴¹ where the self-energy is calculated by the electron propagator (G) and the screened Coulomb interaction (W), by the variational analysis for the effective Wannier equation,⁴² and by calculating the exchange and correlation energies.^{34,43} These theories agree with the experimental data for indirect band-gap materials³⁴ and the semiconductor quantum wires consisting of the III-V materials.⁴¹ The present analysis reveals that the macroscopic coherence generation plays an important role and the conventional theories break down in materials with large exciton binding energy.

We comment that the considerable deviation with the experimental data of Ref. 23 arises from the finite-size effect and from the complex sample geometry. In fact, the sample that was used in the experiment consists of many self-assembled crystallites grown on the sapphire substrate as shown in the atomic-force microscopy image in Ref. 23.

B. The e - h pair correlation and the BCS-like energy-gap formation

The BCS-like energy-gap formation makes a significant contribution not merely to the band-gap reduction but also to the several remarkable characteristics of luminescence spec-

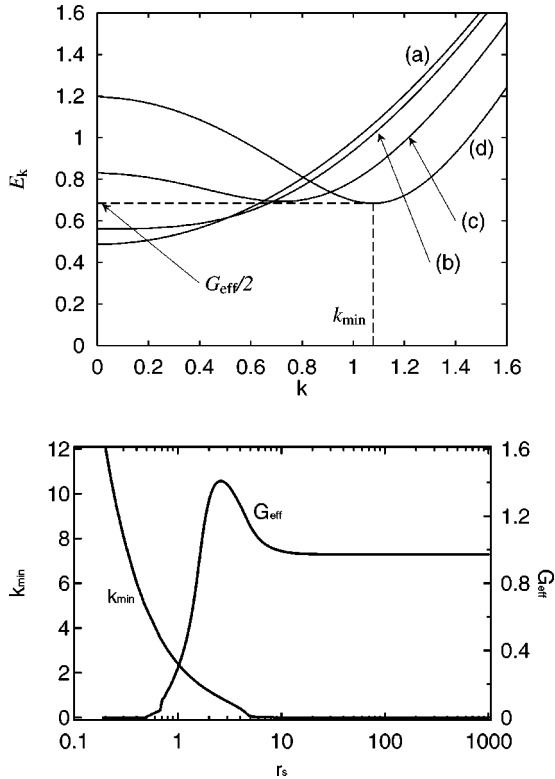


FIG. 2. The upper graph shows the dispersion relation of the single-quasiparticle energy for (a) $r_s = 17$, (b) $r_s = 5.2$, (c) $r_s = 3.0$, and (d) $r_s = 2.2$, and the definition of k_{min} and G_{eff} for $r_s = 2.2$. The lower graph depicts k_{min} and G_{eff} as a function of r_s .

tra as will be discussed in Sec. III C. We discuss in this subsection the BCS-like energy-gap formation by analyzing the r_s dependence of the Bogoliubov quasiparticle energy E_k . As shown in the upper graph of Fig. 2, E_k is characterized by G_{eff} and k_{min} ; here G_{eff} is defined by Eq. (30) and k_{min} is the momentum at which $2E_k$ equals G_{eff} . These quantities are measures of the BCS-BEC crossover that is the main subject of the present study. In low e - h densities, E_k shows the parabolic dispersion with $G_{\text{eff}} = 1$ (the exciton binding energy) and $k_{\text{min}} = 0$. In high e - h densities, E_k exhibits the mexican-hat shape dispersion with G_{eff} and k_{min} equaling the BCS-like energy gap and the quasi-Fermi momentum, respectively.

We show in the lower graph of Fig. 2 the calculated G_{eff} and k_{min} as a function of r_s . We find that $k_{\text{min}} > 0$ for $r_s \lesssim 5$, and G_{eff} considerably different from the exciton binding energy for $r_s \lesssim 10$. These results indicate that the system is in the e - h BCS state for $r_s \lesssim 5$, where the electrons and holes are in Fermi degeneracy because of the Pauli exclusion principle and the BCS-like energy gap is formed at the quasi-Fermi level as shown in the upper graph of Fig. 2. On the contrary, the e - h pairs behave as excitons for $r_s \gtrsim 10$, and the crossover between e - h Cooper pairs and excitons are found in $5 \lesssim r_s \lesssim 10$; these results are consistent with those in Sec. III A.

We also find that the strong screening effect considerably reduces G_{eff} for $r_s < 2$. However, this behavior does not imply that the e - h pair correlation is absent in high e - h densi-

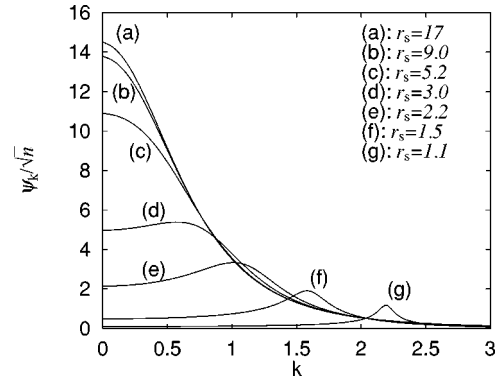


FIG. 3. The wave function of an e - h pair with zero center-of-mass momentum for various r_s .

ties; in fact, the coherent emission from the e - h BCS state is found even in high e - h densities as will be discussed in Sec. III C. This result is found only for sufficiently low temperatures, and the finite temperature effects will be discussed in a forthcoming paper.²⁷ Recently, the authors have shown that, even in very high densities, the e - h pair correlation is enhanced by a strong photoexcitation and the BCS-like gap extraordinarily grows with increasing pump-light intensity.⁴⁴ This result suggests a possibility of decisive experimental observation of e - h BCS state under strong photoexcitations.

Figure 3 illustrates the e - h pair wave function ψ_k (Refs. 6,8,28,29,31) with zero center-of-mass momentum for various r_s . The functional shape of ψ_k also reflects the BCS-BEC crossover. For $r_s \gtrsim 10$, the wave function is a Lorentzian that is the same as that of a $1S$ exciton. For $r_s \lesssim 10$, the wave function deforms because of the quasi-Fermi surface formation, and ψ_k has a maximum point with nonzero momentum that equals k_{min} in $r_s \lesssim 5$. We also find that the normalized wave function ψ_k/\sqrt{n} (n is the e - h density) is nearly independent of r_s for $r_s \gtrsim 10$, and it abruptly reduces for $r_s \lesssim 10$. This reduction indicates that, in high e - h densities, the high quasi-Fermi level formation reduces the fraction of the e - h pairs that contribute to the e - h Cooper pair formation. As shown in Secs. III C and III D, this reduction of the normalized wave function leads to the saturation of the peak intensities of luminescence spectra.

C. Luminescence spectra

We are now in a position to discuss the luminescence spectra for various e - h densities. In the present theory, the luminescence spectra are calculated using Eq. (16) by numerically solving the BS equation (27). We should remark that the singularity-removal method^{40,45} is inappropriate because the singular points of the correlation function considerably depend on the e - h density. We therefore evaluate the eigenvalues and eigenvectors of the stability matrix^{7,46} of the BS kernel to obtain the numerical solution of Eq. (27). This approach enforces us to deal with a giant matrix (about 3000×3000 in dimension) to obtain good overall accuracy. We employ dynamical memory allocation and deallocation in FORTRAN 90 to effectively use the memory space in computers.

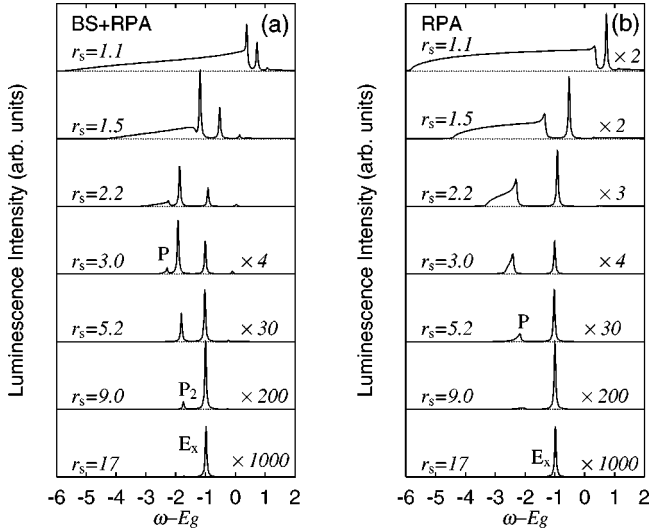


FIG. 4. The luminescence spectra for various r_s given (a) by the present theory, and (b) by the GRPA.

Figures 4(a) shows the luminescence spectra obtained by the present theory. As a reference, we also show in Figs. 4(b) and 5(a) the luminescence spectra given by the GRPA analysis and by the BCS-like mean-field analysis, respectively. In the GRPA analysis, we solve Eq. (27) by neglecting the second term on the left-hand side; in the BCS-like the mean-field theory, we solve Eq. (27) by neglecting the second term on both sides. In Figs. 4 and 5, the exciton decay constant γ is chosen to be 0.03, which gives the sufficient resolution for each spectral components.

In the high e - h density ($r_s = 1.1$), the present theory gives a broad emission band with large band-gap renormalization below the coherent emission line at $\omega - E_g \approx 0.8$. We find a

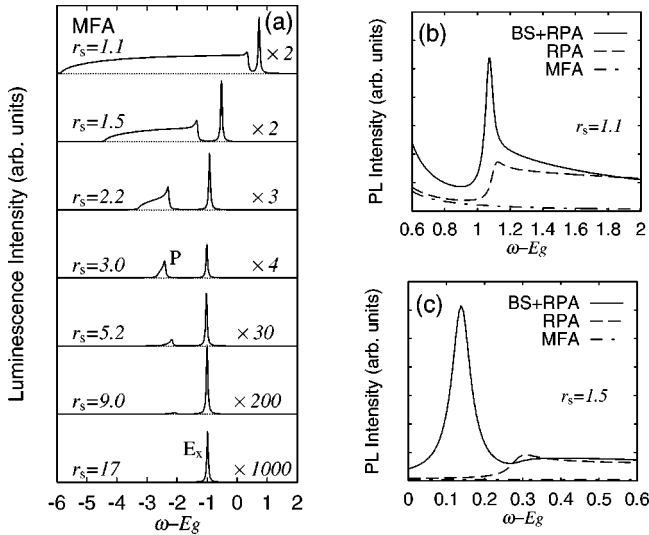


FIG. 5. (a) The luminescence spectra for various r_s given by the BCS-like mean-field theory. (b) and (c) show the enlarged figure above the quasichemical potential for $r_s = 1.1$ and $r_s = 1.5$, respectively. The solid line, the dashed line, and the dashed-dotted line are results given by the present theory, GRPA analysis, and the BCS-like mean-field theory, respectively.

sharp peaked structure at the high-frequency edge of the broad emission band; this structure originates from the singular behavior of the density of states associated with the BCS-like gap formation at the quasi-Fermi level. This peaked structure is strongly pronounced in the present theory because the strong e - h pair correlation described by the second term on the right-hand side of Eq. (27) is considered in the present numerical calculation. We also find that the low-energy edge of the broad emission band in Fig. 4(a) does not exhibit the ordinary square-root shape. This behavior arises from the reduction of the oscillator strength of e - h pairs at the renormalized band edge due to the localization of the oscillator strength at the peaked structure mentioned above. As clearly shown in Figs. 5(b) and 5(c), the present theory predicts a weak emission line above the coherent emission line that originates from the collective phase fluctuation from the e - h BCS state. This component arises from the second term on the right-hand side of Eq. (27); therefore this structure is also found in the GRPA analysis but missing in the BCS-like mean-field analysis. We should remark that electrons and holes are excited above the quasichemical potential by the collective phase fluctuation even at zero temperature.

As shown in the spectra for $r_s = 1.5$ and $r_s = 2.2$, the present theory shows that the broad emission band in $r_s = 1.1$ splits into the broad and the sharp spectral components as the e - h density decreases. With further decrease in the e - h density, the broad spectral component at $\omega - E_g < -2$ sharpens and is assigned to the P line; the sharp component at $\omega - E_g \approx -1.7$ is assigned to the P_2 line. The P line originates from the radiative exciton recombination accompanied by the dissociation of another exciton; the P_2 line originates from the radiative exciton recombination accompanied by the excitation of another exciton from $1S$ to $2S$ state. The P_2 line is obtained by solving the BS equation that considers the strong e - h pair correlation; it should be remarked that neither the GRPA analysis nor the BCS-like mean-field analysis gives the P_2 line. We find for $r_s < 1.5$ the peak intensity of the coherent emission and P_2 lines saturate and weaken with increasing e - h density, and similar saturation is observed in the GaAs and CdSe quantum dot systems.⁴⁷ As discussed in Sec. III B, this behavior arises from the quasi-Fermi surface formation, so that conventional theories based on the interacting Boson model, on the BCS-like mean-field theory, and on the two-electrons and two-holes model⁴⁸ cannot explain this saturation.

As discussed in Sec. III A, we find a reduction of the renormalized band edge as the e - h density decreases. With increasing e - h density, small redshifts in the coherent emission, P and P_2 lines are found, and this behavior is consistent with the experimental result in Ref. 49; the dependence of each spectral position on e - h density will be discussed in detail in Sec. III D.

As shown in the spectra for $r_s = 5.2$, 9.0, and 17 in Fig. 4(a), the present theory also describes very well the low-density properties of luminescence spectra. Namely, the intensities of the coherent emission and P_2 lines show the linear and the quadratic density dependences, respectively, and the coherent emission prevails over any other spectral components in the low-density limit. For $r_s \gtrsim 5$, the coherent

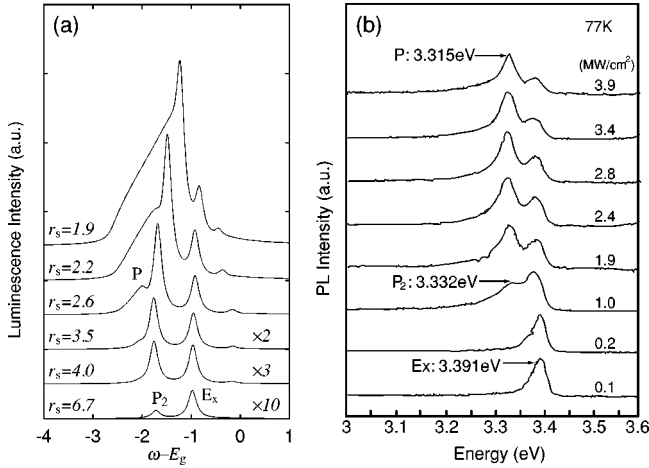


FIG. 6. Comparison between (a) the present theory and (b) the experiment for ZnO thin film at 77 K (from Ref. 26). Here Ex stands for the free exciton emission.

emission line at $\omega - E_g = -1$ is regarded as the exciton luminescence (Ex) line from the $e-h$ BCS state whose linewidth is determined only by its decay rate γ as shown in Eq. (19a).

Now, let us compare the calculated spectra with experimental results. Figure 6 depicts the luminescence spectra given by the present theory and by the experiment for ZnO thin film with thickness $1.3 \mu\text{m}$ at $T = 77 \text{ K}$.²⁶ In Fig. 6(a), the exciton decay constant is chosen as $\gamma = 0.1$. We find that the following properties of the experimental results are well described by the present theory. In the high-density state, a broad emission band appears below the Ex line, and the intensity of the broad band is stronger than that of the Ex line. As the $e-h$ density decreases, the intensity of the broad band superlinearly reduces, and it splits into P and P_2 lines. With further decrease in the $e-h$ density, the intensity of the P line becomes weak and the Ex line predominates over the P_2 line. Unlike conventional two-electrons and two-holes model,⁴⁸ the present many-body theory first enables us to simultaneously evaluate the line-shape and the spectral position for various $e-h$ densities.

D. The luminescence intensity and the spectral position as functions of the $e-h$ density

We discuss the dependence of the luminescence intensity on the $e-h$ density. Figure 7 depicts the peak intensity of the coherent emission, P , P_2 , and P_3 lines as a function of the normalized density n . The P_3 line arises from the exciton recombination accompanied by the excitation of another exciton from $1S$ to $3S$ state; this spectral component is too weak to be found in Fig. 4(a). As discussed in Sec. III C, the coherent emission (luminescence from the exciton BEC state) predominates in low-density states; with increasing $e-h$ density, the P_2 line superlinearly grows and it prevails for $n \geq 1.5 \times 10^{-2}$ ($r_s \leq 4$). For $n \leq 1.5 \times 10^{-2}$, the peak intensity of P_2 -line quadratically depends on n because it arises from the exciton-exciton interaction, while the peak intensity of the coherent emission linearly depends on n .

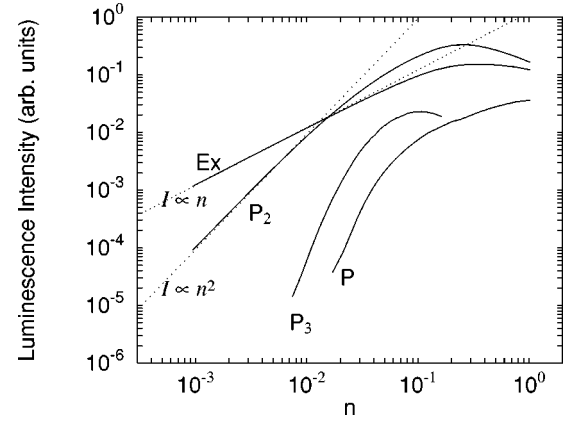


FIG. 7. The density dependence of the peak intensities of the coherent exciton emission (Ex), P_2 , P_3 , and P lines.

These lines saturate for $n \geq 1.5 \times 10^{-2}$ because of the many-body effect. That is, $e-h$ pairs considerably overlap with each other and the fermionic nature of electrons and holes becomes significant. The $e-h$ pairing is therefore restricted near the quasi-Fermi level, which results in the saturation of the coherent emission and the P line.

We show in Fig. 8 the r_s dependence of the spectral position of each spectral component. In low densities ($r_s \geq 10$), the calculated spectral positions of the coherent emission, P_2 and P_3 lines are given by $\omega - E_g = -1$, $-2 - (1/2^2)$ and $-2 + (1/3^2)$, respectively, as expected. In the present theory, the coherent emission and P_2 line show weak redshift for $3 \lesssim r_s \lesssim 10$; this behavior was experimentally observed in Ref. 49. With further increase in the $e-h$ density, all the spectral components show the blueshift for $r_s \lesssim 3$ because of the state-filling effect.

IV. CONCLUSION

We have presented a many-body theory of luminescence spectra for high-density $e-h$ systems, which is applicable throughout the whole densities including the $e-h$ BCS state in very high $e-h$ density and the excitonic BEC state in relatively low $e-h$ density. The analysis is based on the BCS-like pairing theory combined with the BS equation for the $e-h$

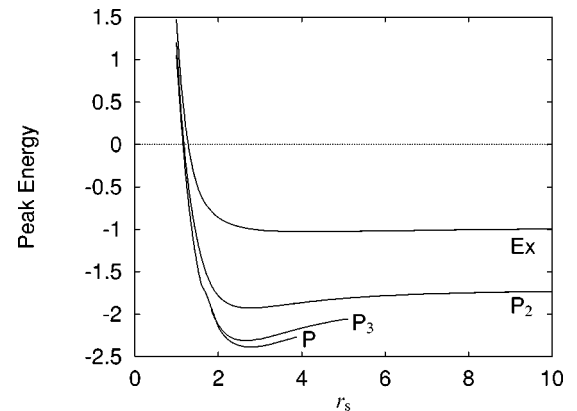


FIG. 8. The r_s dependence of the spectral position of the coherent exciton emission (Ex), P_2 , P_3 , and P lines.

pair-correlation function. This approach first allows us to evaluate the optical spectra by considering the Fermionic nature of electrons and holes and the Bosonic nature of bound e - h pairs. The calculated luminescence spectra and the renormalized band-gap agree very well with experiments as mentioned in Sec. III.

We have clarified the crossover between the e - h BCS state and the excitonic BEC from a unified viewpoint. In particular, we find that the broad emission band from the e - h BCS state splits into two spectral components with decreasing e - h density; these spectral components correspond to the P and P_2 lines in low densities. This behavior well explains the experiment for ZnO thin film in the weak confinement condition.²⁶ In addition, we have calculated the deviation of linear (quadratic) density dependence of the intensity of coherent emission (P_2) line in the wide density range. It should be noted that this deviation of density dependence as well as the blueshift of the P and P_2 lines cannot be explained with the simple two-exciton (two-exciton and two-hole) model, and the present many-body theory makes it possible to incorporate these effects arising from the simultaneously interacting many e - h pairs. These results are important not only in basic physics but also in applied research areas because the ultraviolet laser emission for the P line in ZnO thin films was realized at room temperatures.²² Our analytical method and obtained results will also stimulate renewed interest in the BCS-BEC crossover problem in a variety of physical contexts such as the high- T_c superconductivity where the coherence length is the same order as the main interparticle distance.

Finally, we should pay attention to the important observation that the calculated large band-gap reduction in high densities arises not only from the usual electron/hole exchange interaction but also from the BCS-like energy-gap formation. Whereas no adjustable parameters are introduced in the present theory, the calculated result shows excellent agreement with experiments and shows the universal behavior for bulk CuCl (Ref. 25) and ZnO (Ref. 24) thin film in the weak confinement condition. This fact indicates that the spontaneously generated macroscopic quantum state is actually generated in highly photoexcited semiconductors.^{24,25}

ACKNOWLEDGMENTS

The authors thank Professor M. Kuwata-Gonokami, Dr. M. Nagai, and Dr. A. Yamamoto for valuable information on experiments. One of the author (T.J.I.) thanks Professor D. A. Worman for valuable comments on the manuscript. This work is partially supported by a Grant-in-Aid for Scientific Research on priority areas, ‘‘Photo-induced Phase Transition and Their Dynamics’’ from the Ministry of Education, Science, Culture and Sports of Japan.

APPENDIX A: THE SEMICONDUCTOR ANDERSON-RICKAYZEN EQUATION

In this paper, we consider a collective phase fluctuation associated with the center-of-mass motion of e - h pairs by the generalized random-phase approximation.²⁰ For this purpose,

we calculate the semiconductor version of the Anderson-Rickayzen equation (SCARE), which is the linearized equation of motion for the bilinear products of the Bogoliubov quasiparticle operators,

$$\begin{aligned}\Psi_0^q(\mathbf{k}) &= \alpha_k^\dagger \alpha_{q+\mathbf{k}} = \frac{1}{2}[\Phi_0^q(\mathbf{k}) + \Phi_3^q(\mathbf{k})], \\ \Psi_1^q(\mathbf{k}) &= \alpha_k^\dagger \beta_{-q-\mathbf{k}}^\dagger = \frac{1}{2}[\Phi_1^q(\mathbf{k}) + i\Phi_2^q(\mathbf{k})], \\ \Psi_2^q(\mathbf{k}) &= \beta_{-q-\mathbf{k}} \alpha_{q+\mathbf{k}} = \frac{1}{2}[\Phi_1^q(\mathbf{k}) - i\Phi_2^q(\mathbf{k})], \\ \Psi_3^q(\mathbf{k}) &= \beta_{-q-\mathbf{k}} \beta_{-q-\mathbf{k}}^\dagger = \frac{1}{2}[\Phi_0^q(\mathbf{k}) - \Phi_3^q(\mathbf{k})].\end{aligned}\quad (\text{A1})$$

Here the $j=0,3$ and $j=1,2$ components of $\Psi_j^q(\mathbf{k})$ describe the density and phase fluctuation from the e - h BCS state, respectively. The SCARE is written as follows:

$$[\Psi_0^{q\dagger}(\mathbf{k}), H] = -(E_{k+q} - E_k) \Psi_0^{q\dagger}(\mathbf{k}), \quad (\text{A2a})$$

$$\begin{aligned}[\Psi_1^{q\dagger}(\mathbf{k}), H] &= (E_{k+q} + E_k) \Psi_1^{q\dagger}(\mathbf{k}) \\ &+ C_{k,k+q}^{(3)} V_q \sum_p C_{p,p+q}^{(3)} [\Psi_1^{q\dagger}(\mathbf{p}) - \Psi_2^{q\dagger}(\mathbf{p})],\end{aligned}\quad (\text{A2b})$$

$$\begin{aligned}[\Psi_2^{q\dagger}(\mathbf{k}), H] &= -(E_{k+q} + E_k) \Psi_2^{q\dagger}(\mathbf{k}) \\ &+ C_{k,k+q}^{(3)} V_q \sum_p C_{p,p+q}^{(3)} [\Psi_1^{q\dagger}(\mathbf{p}) - \Psi_2^{q\dagger}(\mathbf{p})],\end{aligned}\quad (\text{A2c})$$

$$[\Psi_3^{q\dagger}(\mathbf{k}), H] = (E_{k+q} - E_k) \Psi_3^{q\dagger}(\mathbf{k}), \quad (\text{A2d})$$

where we only keep the terms that give the leading contribution in the $\mathbf{q} \rightarrow \mathbf{0}$ limit. In deriving the SCARE, we replace the products of Ψ 's by their expectation values with respect to the ground state in the full equations of motion for Ψ 's. Equations (A2a) and (A2d) show that $\Psi_j^q(\mathbf{k})$ ($j=0,3$), is an eigenoperator with eigenvalues $(-1)^{j+1}(E_{k+q} - E_k)$, and $\Psi_j^q(\mathbf{k})$ ($j=1,2$) describes the scattering of excitations that are already present in the initial state. Equation (A2) indicates that $\Psi_j^q(\mathbf{k})$ with $j=0,3$ and $\mathbf{q} \neq \mathbf{0}$ is irrelevant at zero temperature because no Bogoliubov quasiparticles are created by $\Psi_j^q(\mathbf{k})$ with $j=0,3$ and $\mathbf{q} \neq \mathbf{0}$. In Ref. 20, these operators are called unphysical because all the physical states satisfy

$$\Psi_j^{q\dagger}(\mathbf{k})|\text{phys}\rangle = 0, \quad (\text{A3})$$

for $j=0,3$. The absence of these operators in the present theory is confirmed by Eqs. (19a) and (20).

APPENDIX B: EVALUATION OF Eq. (20)

In this Appendix, we evaluate the intensity of the coherent emission, I_{coh} , given in Eq. (20). For this purpose, we use the following operator identity:

$$\begin{aligned} \Phi_{\mu}^{0\dagger}(\mathbf{p})\Phi_{\nu}^0(\mathbf{k}) &= -\frac{1}{4}\text{tr}(\boldsymbol{\tau}_{\mu}\boldsymbol{\tau}_{\rho}\boldsymbol{\tau}_{\nu}\boldsymbol{\tau}_{\sigma})\Phi_{\sigma}^{p-k\dagger}(\mathbf{k})\Phi_{\rho}^{p-k}(\mathbf{k}) \\ &\quad +\frac{1}{2}\delta_{p,k}\text{tr}(\boldsymbol{\tau}_{\mu}\boldsymbol{\tau}_{\nu}\boldsymbol{\tau}_{\rho})\Phi_{\rho}^0(\mathbf{p})+2\delta_{k,p}\delta_{\nu,0}\Phi_{\mu}^0(\mathbf{p}). \end{aligned} \quad (\text{B1})$$

Substituting Eq. (B1) into the second term on the right-hand side of Eq. (19c), we obtain

$$\begin{aligned} &\sum_{j=1}^2\sum_{k,p}g_k^*g_p\{\mathbf{K}_{k,j}^{\dagger}\langle\Phi_j^{0\dagger}(\mathbf{k})\Phi_3^0(\mathbf{p})\rangle_0\mathbf{K}_{p,3}+\text{c.c.}\} \\ &= -\frac{1}{8}\sum_{k,p}g_k^*g_p\{i\langle[\Phi_2^{k-p\dagger}(\mathbf{p}),\Phi_3^{k-p}(\mathbf{p})]\rangle_0(C_{k,k}^{(1)}-C_{p,p}^{(1)}) \\ &\quad +\langle[\Phi_1^{k-p\dagger}(\mathbf{p}),\Phi_0^{k-p}(\mathbf{p})]\rangle_0(C_{k,k}^{(1)}+C_{p,p}^{(1)}) \\ &\quad +i\langle\{\Phi_2^{k-p\dagger}(\mathbf{p}),\Phi_0^{k-p}(\mathbf{p})\}\rangle_0(C_{k,k}^{(2)}C_{p,p}^{(1)}-C_{k,k}^{(1)}C_{p,p}^{(2)}) \\ &\quad +\langle\{\Phi_3^{k-p\dagger}(\mathbf{p}),\Phi_1^{k-p}(\mathbf{p})\}\rangle_0(C_{k,k}^{(2)}C_{p,p}^{(1)}+C_{k,k}^{(1)}C_{p,p}^{(2)})\}=0, \end{aligned} \quad (\text{B2})$$

where we used the fact that $\Phi_j^q(\mathbf{p})$ ($j=0,3$) is the eigenoperator and

$$[\Phi_j^{q\dagger}(\mathbf{k}),\Phi_m^q(\mathbf{k})]=0 \quad (\text{B3})$$

for $j=0,3$ and $m=1,2$.

Therefore, we obtain the following expression for Eq. (19c):

$$\begin{aligned} I_{\text{coh}} &= \frac{1}{2}\sum_{k,p}g_k^*g_p\mathbf{K}_{k,3}^{\dagger}\langle\Phi_3^{0\dagger}(\mathbf{k})\Phi_3^0(\mathbf{p})\rangle_0\mathbf{K}_{p,3} \\ &= \frac{1}{8}\sum_{k,p}g_k^*g_pC_{k,k}^{(1)}C_{p,p}^{(1)}\left\{2\delta_{k,p} \right. \\ &\quad \left. +\sum_{j=1,2}\langle\Phi_j^{p-k\dagger}(\mathbf{k})\Phi_j^{p-k}(\mathbf{k})\rangle_0\right\}, \end{aligned} \quad (\text{B4})$$

where we used Eq. (B1) to obtain the last expression for Eq. (B4).

APPENDIX C: EVALUATION OF $\langle\Phi^{p-k\dagger}(\mathbf{k})\boldsymbol{\tau}_{\mu}\Phi^{p-k}(\mathbf{k})\rangle_0$

In this Appendix, we calculate $\langle\Phi^{q\dagger}(\mathbf{k})\boldsymbol{\tau}_{\mu}\Phi^q(\mathbf{p})\rangle_0$ for $\mu=0,3$ with the generalized RPA. We first introduce the two-particle Green function by

$$i[\mathbf{G}^q(\mathbf{k},\mathbf{p},t)]_{j,m}=\langle T\Phi_j^{q\dagger}(\mathbf{k},t)\Phi_m^q(\mathbf{p},0)\rangle_0, \quad (\text{C1})$$

where T stands for chronological ordering. The expectation value is expressed by the equal-time limit of the Green function,

$$\begin{aligned} \langle\Phi^{p-k\dagger}(\mathbf{k})\boldsymbol{\tau}_{\mu}\Phi^{p-k}(\mathbf{k})\rangle_0 &= i\lim_{t\rightarrow\delta}\text{tr}\{\boldsymbol{\tau}_{\mu}\mathbf{G}^{p-k}(\mathbf{k},\mathbf{k},t)\} \\ &= i\int_{-\infty}^{\infty}\frac{d\omega}{2\pi}e^{-i\omega\delta}\text{tr}\{\boldsymbol{\tau}_{\mu}\mathbf{G}^{p-k}(\mathbf{k},\mathbf{k},\omega)\}, \end{aligned} \quad (\text{C2})$$

where δ is the infinitesimal positive number, and $\mathbf{G}^q(\mathbf{k},\mathbf{p},\omega)$ is the Fourier transform of $\mathbf{G}^q(\mathbf{k},\mathbf{p},t)$.

The equation of motion for $\mathbf{G}^q(\mathbf{k},\mathbf{p},t)$ is obtained by the SCARE, Eqs. (A2), and the result is written as follows:

$$\begin{aligned} &\left(i\frac{\partial}{\partial t}\boldsymbol{\tau}_0-\boldsymbol{\varepsilon}_k^q\boldsymbol{\tau}_2\right)\mathbf{G}^q(\mathbf{k},\mathbf{p},t)+iC_{k,k+q}^{(3)} \\ &\quad \times(\boldsymbol{\tau}_1+i\boldsymbol{\tau}_2)V_q\sum_{k'}C_{k',k'+q}^{(3)}\mathbf{G}^q(\mathbf{k}',\mathbf{p},t)=2\delta_{k,p}\boldsymbol{\tau}_2, \end{aligned} \quad (\text{C3})$$

where $\boldsymbol{\varepsilon}_k^q=E_{k+q}+E_k$. We can analytically solve Eq. (C3) by introducing the auxiliary function defined by

$$\boldsymbol{\eta}^{q\dagger}(\mathbf{p},t)=V_q\sum_kC_{k,k+q}^{(3)}\boldsymbol{e}_2^{\dagger}\mathbf{G}^q(\mathbf{k},\mathbf{p},t), \quad (\text{C4})$$

where $\boldsymbol{e}_1=(1,0)$ and $\boldsymbol{e}_2=(0,1)$. Using an identity, $\boldsymbol{\tau}_1+i\boldsymbol{\tau}_2=2\boldsymbol{e}_1\otimes\boldsymbol{e}_2^{\dagger}$, we find that the solution of Eq. (C3) is written as follows:

$$\begin{aligned} \mathbf{G}^q(\mathbf{k},\mathbf{p},\omega) &= 2\delta_{k,p}\boldsymbol{\tau}_2\left(\frac{\omega\boldsymbol{\tau}_0+\boldsymbol{\varepsilon}_k^q\boldsymbol{\tau}_2}{\omega^2-(\boldsymbol{\varepsilon}_k^q)^2}\right) \\ &\quad +2\mathcal{V}_q(\omega)C_{k,k+q}^{(3)}C_{p,p+q}^{(3)}\left(\frac{\omega\boldsymbol{\tau}_0+\boldsymbol{\varepsilon}_k^q\boldsymbol{\tau}_2}{\omega^2-(\boldsymbol{\varepsilon}_k^q)^2}\right) \\ &\quad \times(\boldsymbol{\tau}_1+i\boldsymbol{\tau}_2)\left(\frac{\omega\boldsymbol{\tau}_2+\boldsymbol{\varepsilon}_p^q\boldsymbol{\tau}_0}{\omega^2-(\boldsymbol{\varepsilon}_p^q)^2}\right), \end{aligned} \quad (\text{C5a})$$

where $\mathcal{V}_q(\omega)=V_q/[1+V_q\Pi_q(\omega)]$ is the screened Coulomb potential given by the polarization function $\Pi_q(\omega)$,

$$\Pi_q(\omega)=-2\sum_k\frac{\boldsymbol{\varepsilon}_k^qC_{k,k+q}^{(3)2}}{\omega^2-(\boldsymbol{\varepsilon}_k^q)^2}. \quad (\text{C5b})$$

Substituting Eqs. (C5a) into right-hand side of Eq. (C2), we obtain

$$\begin{aligned} &\langle\Phi^{p-k\dagger}(\mathbf{k})\boldsymbol{\tau}_0\Phi^{p-k}(\mathbf{k})\rangle_0 \\ &= 2+2i\int_{-\infty}^{\infty}\frac{d\omega}{\pi}\mathcal{V}_{k-p}(\omega)C_{k,p}^{(3)2}\frac{\omega^2+(E_k+E_p)^2}{\{\omega^2-(E_k+E_p)^2\}^2}, \end{aligned} \quad (\text{C6a})$$

$$\langle\Phi^{p-k\dagger}(\mathbf{k})\boldsymbol{\tau}_3\Phi^{p-k}(\mathbf{k})\rangle_0=2i\int_{-\infty}^{\infty}\frac{d\omega}{\pi}\frac{\mathcal{V}_{k-p}(\omega)C_{k,p}^{(3)2}}{\omega^2-(E_k+E_p)^2}. \quad (\text{C6b})$$

In Eqs. (C6), the integral with respect to ω is calculated by introducing the spectral-weight function of dielectric function $B_q(\omega)$ given by

$$B_q(\omega)=-i\{\boldsymbol{\varepsilon}_q^{-1}(\omega-i\delta)-\boldsymbol{\varepsilon}_q^{-1}(\omega+i\delta)\}. \quad (\text{C7})$$

The dielectric function, $\boldsymbol{\varepsilon}_q(\omega)=1+V_q\Pi_q(\omega)$, satisfies the dispersion relation,

$$\frac{1}{\epsilon_q(\omega)} = 1 - \int_0^\infty \frac{dz}{\pi} \frac{z B_q(z)}{\omega^2 - z^2}. \quad (\text{C8})$$

We can evaluate the integral with respect to ω in Eq. (C6) using Eq. (C8), and the result is

$$\langle \Phi^{p-k^\dagger}(\mathbf{k}) \tau_0 \Phi^{p-k}(\mathbf{k}) \rangle_0 = 2 - 8 C_{k,p}^{(3)2} V_{k-p} \left[\frac{\partial \chi_{k-p}(\omega)}{\partial \omega} \right]_{\omega = -E_k - E_p}, \quad (\text{C9a})$$

$$\begin{aligned} & \langle \Phi^{p-k^\dagger}(\mathbf{k}) \tau_3 \Phi^{p-k}(\mathbf{k}) \rangle_0 \\ &= \frac{2 V_{k-p} C_{k,p}^{(3)2}}{E_k + E_p} [1 + 2 \chi_{k-p}(-E_k - E_p)], \end{aligned} \quad (\text{C9b})$$

where $\chi_q(\omega)$ is the partial screening function³⁰ defined by

$$\chi_q(\omega) = \int_0^\infty \frac{dz}{2\pi} \frac{B_q(z)}{z - \omega}. \quad (\text{C10})$$

*Electronic address: inagaki@ms.aist-nara.ac.jp

¹S. A. Moskalenko and D. W. Snoke, *Bose-Einstein Condensation of Excitons and Biexcitons* (Cambridge University Press, Cambridge, 2000).

²A. E. Bulatov and S. G. Tikhodeev, Phys. Rev. B **46**, 15 058 (1992); G. A. Kopelevich, N. A. Gippius, and S. G. Tikhodeev, Solid State Commun. **99**, 93 (1996); S. G. Tikhodeev, Phys. Rev. Lett. **78**, 3225 (1997); S. G. Tikhodeev, G. A. Kopelevich, and N. A. Gippius, Phys. Status Solidi B **206**, 45 (1998).

³E. Fortin, S. Fafard, and A. Mysyrowicz, Phys. Rev. Lett. **70**, 3951 (1993); A. Mysyrowicz, E. Benson, and E. Fortin, *ibid.* **77**, 896 (1996).

⁴H. Kondo, T. Kawai, and T. Karasawa, Solid State Commun. **94**, 129 (1995); H. Kondo, T. Kawai, T. Karasawa, I. Akai, and T. Komatsu, J. Lumin. **66&67**, 448 (1996); H. Mino, T. Kawai, I. Akai, and T. Karasawa, *ibid.* **76&77**, 109 (1998); H. Kondo, H. Mino, I. Akai, and T. Karasawa, Phys. Rev. B **58**, 13 835 (1998); T. Karasawa, H. Mino, and M. Yamamoto, J. Lumin. **87-89**, 174 (2000).

⁵E. Hanamura and H. Haug, Phys. Lett. C **33**, 209 (1977).

⁶L. V. Keldysh and Yu. V. Kopaev, Fiz. Tverd. Tela **6**, 2791 (1964) [Sov. Phys. Solid State **6**, 2219 (1965)]; L. V. Keldysh and A. N. Kozlov, Zh. Eksp. Teor. Fiz. **54**, 978 (1968), [Sov. Phys. JETP **27**, 521 (1968)]; C. Comte and P. Nozières, J. Phys. (Paris) **43**, 1069 (1982); P. Nozières and C. Comte, *ibid.* **43**, 1083 (1982); C. Comte and G. Mahler, Phys. Rev. B **34**, 7164 (1986).

⁷T. J. Inagaki, M. Aihara, and A. Takahashi, Solid State Commun. **115**, 645 (2000).

⁸P. Nozières and S. Schmitt-Rink, J. Low Temp. Phys. **59**, 195 (1985).

⁹Y. Wada, Prog. Theor. Phys. **24**, 920 (1960); **25**, 713 (1961); **26**, 321 (1961).

¹⁰A. J. Leggett, in *Modern Trends in the Theory of Condensed Matter*, edited by A. Pękalski and J. Przystawa (Springer-Verlag, Berlin, 1980), p. 14.

¹¹As a review on BCS-BEC crossover before 1994, see, for example, M. Randeria, in *Bose-Einstein Condensation*, edited by A. Griffin, D. W. Snoke, and S. Stringari (Cambridge University Press, Cambridge, 1995), p. 355.

¹²A. Tokumitsu, K. Miyake, and Kazuo Yamada, Phys. Rev. B **47**, 11 988 (1993); F. Pistolesi and G. C. Strinati, *ibid.* **49**, 6356 (1994); R. Haussmann, *ibid.* **49**, 12 975 (1994); F. Pistolesi and G. C. Strinati, *ibid.* **53**, 15 168 (1996); N. Andrenacci, A. Perali, P. Pieri, and G. C. Strinati, *ibid.* **60**, 12 410 (1999); J. P. Wallington and J. F. Annett, *ibid.* **61**, 1433 (2000); P. Pieri and G. C. Strinati, *ibid.* **61**, 15 370 (2000); P. Pieri, G. C. Strinati, and I.

Tifrea, *ibid.* **64**, 052104 (2001); K. Yamada, S. Koikegami, Y. Yanase, T. Jujo, and T. Nomura, J. Phys. Chem. Solids **62**, 75 (2001); Y. Yanase and K. Yamada, J. Phys. Soc. Jpn. **68**, 548 (2000); T. Nomura and K. Yamada, *ibid.* **69**, 3678 (2000); Y. Yanase, T. Jujo, and K. Yamada, *ibid.* **69**, 3664 (2000); Z. Li and K. Yamada, *ibid.* **70**, 797 (2001).

¹³Y. J. Uemura, L. P. Le, G. M. Luke, B. J. Sternlieb, W. D. Wu, J. H. Brewer, T. M. Riseman, C. L. Seaman, M. B. Maple, M. Ishikawa, D. G. Hinks, J. D. Jorgensen, G. Saito, and H. Yamochi, Phys. Rev. Lett. **66**, 2665 (1991); Y. J. Uemura, A. Keren, L. P. Le, G. M. Luke, W. D. Wu, Y. Kubo, T. Manako, Y. Shimakawa, M. Subramanian, J. L. Cobb, and J. T. Markert, Nature (London) **352**, 605 (1991).

¹⁴M. Kira, F. Jahnke, and S. W. Koch, Phys. Rev. Lett. **81**, 3263 (1998).

¹⁵M. Kira, F. Jahnke, and S. W. Koch, Phys. Rev. Lett. **82**, 3544 (1999); K. Hannewald, S. Glutsch, and F. Bechstedt, Phys. Rev. B **62**, 4519 (2000); M. Kira, W. Hoyer, T. Stroucken, and S. W. Koch, Phys. Rev. Lett. **87**, 176401 (2001); K. Hannewald, S. Glutsch, and F. Bechstedt, *ibid.* **86**, 2451 (2001).

¹⁶M. H. Anderson, J. R. Ensher, M. R. Matthews, C. E. Wieman, and E. A. Cornell, Science **269**, 198 (1995); C. C. Bradley, C. A. Sackett, J. J. Tollett, and R. G. Hulet, Phys. Rev. Lett. **75**, 1687 (1995); K. B. Davis, M.-O. Mewes, M. R. Andrews, N. J. van Druten, D. S. Durfee, D. M. Kurn, and W. Ketterle, Phys. Rev. Lett. **75**, 3969 (1995).

¹⁷See, e.g., N. Nakanishi, Suppl. Prog. Theor. Phys. **43**, 1 (1969); Prog. Theor. Phys. Suppl. **95**, 1 (1988).

¹⁸H. Chu and Y. C. Chang, Phys. Rev. B **54**, 5020 (1996); H. Chu and Y. C. Chang, Europhys. Lett. **35**, 535 (1996).

¹⁹S. Glutsch and R. Zimmermann, Phys. Rev. B **45**, 5857 (1992).

²⁰P. W. Anderson, Phys. Rev. **112**, 1900 (1958); G. Rickayzen, *ibid.* **115**, 795 (1959); A. Bardasis and J. R. Schrieffer, *ibid.* **121**, 1050 (1961).

²¹S. Schmitt-Rink and D. S. Chemla, Phys. Rev. Lett. **57**, 2752 (1986); S. Schmitt-Rink, D. S. Chemla, and H. Haug, Phys. Rev. B **37**, 941 (1988); M. Lindberg and S. W. Koch, *ibid.* **38**, 3342 (1988); R. Binder, S. W. Koch, M. Lindberg, W. Schäfer, and F. Jahnke, *ibid.* **43**, 6520 (1991); R. Binder and S. W. Koch, Prog. Quantum Electron. **19**, 307 (1995).

²²Z. K. Tang, G. K. L. Wong, P. Yu. M. Kawasaki, A. Ohtomo, H. Koinuma, and Y. Segawa, Appl. Phys. Lett. **72**, 3270 (1998).

²³P. Zu, Z. K. Tang, G. K. L. Wong, M. Kawasaki, A. Ohtomo, H. Koinuma, and T. Segawa, Solid State Commun. **103**, 459 (1997); P. Yu, Z. K. Tang, G. K. Wong, M. Kawasaki, A. Ohtomo, H. Koinuma, and Y. Segawa, *Proceedings of the 23rd*

- International Conference on the Physics of Semiconductors*, edited by M. Scheffler and R. Zimmermann (World Scientific, Singapore, 1996), Vol. 2, p. 1453.
- ²⁴A. Yamamoto, T. Kido, T. Goto, Y. Chen, T. Yao, and A. Kasuya, *Appl. Phys. Lett.* **75**, 469 (1999); A. Yamamoto, K. Miyajima, T. Goto, H. J. Ko, and T. Yao, *J. Appl. Phys.* **90**, 4973 (2001); A. Yamamoto and K. Miyajima (private communication); A. Yamamoto, K. Miyajima, T. Goto, H. J. Ko, and T. Yao, *J. Lumin.* (to be published).
- ²⁵S. Yamamoto, Master thesis, The University of Tokyo, 1997; M. Nagai, S. Yamamoto, and M. Kuwata-Gonokami (unpublished).
- ²⁶H. J. Ko, Y. F. Chen, Z. Zhu, T. Yao, I. Kobayashi, and H. Uchiki, *Appl. Phys. Lett.* **76**, 1905 (2000).
- ²⁷T. J. Inagaki and M. Aihara (unpublished).
- ²⁸H. Haug and S. Schmitt-Rink, *Prog. Quantum Electron.* **9**, 3 (1988).
- ²⁹J. Zittartz, *Phys. Rev.* **162**, 752 (1967).
- ³⁰R. Zimmermann, *Phys. Status Solidi B* **76**, 191 (1976).
- ³¹T. Iida, Y. Hasegawa, H. Higashimura, and M. Aihara, *Phys. Rev. B* **47**, 9328 (1993).
- ³²J. P. Löwenau, S. Schmitt-Rink, and H. Haug, *Phys. Rev. Lett.* **49**, 1511 (1982).
- ³³Th. Habrich and G. Mahler, *Phys. Status Solidi B* **117**, 635 (1983).
- ³⁴P. Vashishta and R. K. Kalia, *Phys. Rev. B* **25**, 6492 (1982); A. H. Simon, S. J. Kirch, and J. P. Wolfe, *ibid.* **46**, 10 098 (1992).
- ³⁵G. Tränkle, H. Leier, A. Forchel, H. Haug, C. Ell, and G. Weimann, *Phys. Rev. Lett.* **58**, 419 (1987).
- ³⁶S. Nikitine, *Prog. Semicond.* **6**, 269 (1962).
- ³⁷J. Ringeissen and S. Nikitine, *J. Phys. (Paris)* **28**, C3-48 (1967).
- ³⁸D. G. Thomas, *J. Phys. Chem. Solids* **15**, 86 (1960).
- ³⁹R. K. Watts, *Poins Defects in Solids* (Wiley, New York, 1977).
- ⁴⁰H. Haug and S. W. Koch, *Quantum Theory of the Optical and Electronic Properties of Semiconductors*, 3rd ed. (World Scientific, Singapore, 1994).
- ⁴¹I. K. Marmorosk and S. Das Sarma, *Phys. Rev. B* **44**, 3451 (1991); E. H. Hwang and S. Das Sarma, *ibid.* **58**, R1738 (1998).
- ⁴²S. Schmitt-Rink and C. Ell, *J. Lumin.* **30**, 585 (1985).
- ⁴³G. Beni and T. M. Rice, *Phys. Rev. B* **18**, 768 (1978); A. Yamamoto, T. Kido, T. Goto, Y. Chen, and T. Yao, *Int. J. Mod. Phys.* **15**, 3737 (2001).
- ⁴⁴T. J. Inagaki, T. Iida, and M. Aihara, *Phys. Rev. B* **62**, 10 852 (2000).
- ⁴⁵S. Schmitt-Rink, J. P. Löwenau, and H. Haug, *Z. Phys. B: Condens. Matter* **47**, 13 (1982); S. Schmitt-Rink, C. Ell, and H. Haug, *Phys. Rev. B* **33**, 1183 (1986).
- ⁴⁶P. Ring and P. Schuck, *The Nuclear Many-Body Problem* (Springer, New York, 1980).
- ⁴⁷R. Heitz, F. Guffarth, I. Mukhametzhanov, M. Grundmann, A. Madhukar, and D. Bimberg, *Phys. Rev. B* **62**, 16 881 (2000); L. Müller-Kirsch, R. Heitz, A. Schliwa, O. Stier, D. Bimberg, H. Kirmse, and W. Neumann, *Appl. Phys. Lett.* **78**, 1418 (2001); M. Ando, T. J. Inagaki, Y. Kanemitsu, T. Kushida, K. Maehashi, Y. Murase, T. Ota, and H. Nakashima, *J. Lumin.* **94&95**, 403 (2001).
- ⁴⁸T. Moriya and T. Kushida, *J. Phys. Soc. Jpn.* **40**, 1668 (1976); **40**, 1676 (1976); T. Moriya and T. Kushida, *J. Lumin.* **12&13**, 775 (1976); H. Büttner, *Phys. Status Solidi* **42**, 775 (1970).
- ⁴⁹C. Benoit à la Guillaume, J.-M. Debever, and F. Salvan, *Phys. Rev.* **177**, 567 (1969); J. Bille, H. Liebing, and P. Mengel, *Phys. Status Solidi B* **53**, 353 (1972).